

UPR-924-T
BNL-HET-01/3
December 2, 2018
hep-ph/0102083

GigaZ: High Precision Tests of the SM and the MSSM

J. ERLER¹ AND S. HEINEMEYER²

¹*Department of Physics and Astronomy, University of Pennsylvania,
Philadelphia PA 19104-6396, USA*

²*BNL, Physics Department, Upton NY 11973, USA*

The high-energy e^+e^- collider TESLA can be operated in the GigaZ mode on the Z resonance, producing $\mathcal{O}(10^9)$ Z bosons per year. This will allow the measurement of the effective electroweak mixing angle to an accuracy of $\delta \sin^2 \theta_{\text{eff}} \approx \pm 1 \times 10^{-5}$. Similarly the W boson mass is expected to be measurable with an error of $\delta M_W \approx \pm 6$ MeV near the W^+W^- threshold. We discuss the impact of these observables on the accuracy with which the Higgs boson mass can be determined from loop corrections within the Standard Model. We also study indirect constraints on new mass scales within the Minimal Supersymmetric Standard Model.

Presented by JENS ERLER at the

5th International Symposium on Radiative Corrections
(RADCOR-2000)

Carmel CA, USA, 11–15 September, 2000

1 Introduction

The high-energy e^+e^- linear collider TESLA is being designed to operate on top of the Z boson resonance by adding a bypass to the main beam line. Given the high luminosity, $\mathcal{L} = 7 \times 10^{33} \text{cm}^{-2}\text{s}^{-1}$, and the cross section, $\sigma_Z \approx 30 \text{ nb}$, about 2×10^9 Z events can be generated in an operational year of 10^7s . We will therefore refer to this option as the GigaZ mode of the machine. Moreover, by increasing the collider energy to the W -pair threshold, about 10^6 W bosons can be generated at the optimal energy point for measuring the W boson mass, M_W , near threshold and about 3×10^6 W bosons at the energy of maximal cross section. The large increase in the number of Z events by two orders of magnitude as compared to LEP1 and the increasing precision in the measurements of W boson properties, open new opportunities for high precision physics in the electroweak sector [1].

By adopting the Blondel scheme [2], the left-right asymmetry, $A_{LR} \equiv 2(1 - 4\sin^2\theta_{\text{eff}})/(1 + (1 - 4\sin^2\theta_{\text{eff}})^2)$, can be measured with very high precision, $\delta A_{LR} \approx \pm 10^{-4}$ [3], when both, electrons and positrons, are polarized longitudinally. From A_{LR} the mixing angle in the effective leptonic vector coupling of the on-shell Z boson, $\sin^2\theta_{\text{eff}}$, can be determined to an accuracy [3],

$$\delta \sin^2\theta_{\text{eff}} \approx \pm 1 \times 10^{-5}, \quad (1)$$

while the W boson mass is expected to be measurable within [4]

$$\delta M_W \approx \pm 6 \text{ MeV}. \quad (2)$$

Besides the improvements in $\sin^2\theta_{\text{eff}}$ and M_W , GigaZ has the potential to determine the total Z width within $\delta\Gamma_Z = \pm 1 \text{ MeV}$; the ratio of hadronic to leptonic partial Z widths with a relative uncertainty of $\delta R_l/R_l = \pm 0.05\%$; the ratio of the $b\bar{b}$ to the hadronic partial widths with a precision of $\delta R_b = \pm 1.4 \times 10^{-4}$; and to improve the b quark asymmetry parameter A_b to a precision of $\pm 1 \times 10^{-3}$ [3]. These additional measurements offer complementary information on the Higgs boson mass, M_H , but also on the strong coupling constant, α_s , which enters the radiative corrections in many places. This is desirable in its own right, and in the present context it is important to control α_s effects from higher order loop contributions to avoid confusion with Higgs effects. Indirectly, a well known α_s would also help to control m_t effects, since m_t from a threshold scan at a linear collider will be strongly correlated with α_s . We find that via a precise measurement of R_l , GigaZ would provide a clean determination of α_s with small error,

$$\delta\alpha_s \approx \pm 0.001, \quad (3)$$

and consequently a smaller uncertainty in δm_t compared to a linear collider, given identical threshold data ($5 \times 10 \text{ fb}^{-1}$). The anticipated precisions for the most relevant

Table 1: Expected precision at various colliders for $\sin^2\theta_{\text{eff}}$, M_W , m_t and the (lightest) Higgs boson mass, M_H , at the reference value $M_H = 110$ GeV. Run IIA refers to 2 fb^{-1} integrated luminosity per experiment collected at the Tevatron with the Main Injector, while Run IIB assumes the accumulation of 30 fb^{-1} by each experiment. LC corresponds to a linear collider without the GigaZ mode. (The entry in parentheses assumes a fixed target polarized Møller scattering experiment using the e^- beam.) Concerning the present value of M_W some improvement can be expected from the final analysis of the LEP 2 data. δm_t from the Tevatron and the LHC is the error for the top pole mass, while at the top threshold in e^+e^- collisions the $\overline{\text{MS}}$ top-quark mass can be determined. The smaller value of δm_t at GigaZ compared to the LC is due to the prospective reduced uncertainty in α_s , which affects the relation between the mass parameter directly extracted at the top threshold and the $\overline{\text{MS}}$ top-quark mass.

	now	Run IIA	Run IIB	LHC	LC	GigaZ
$\delta \sin^2 \theta_{\text{eff}} (\times 10^5)$	17	50	13	21	(6)	1.3
δM_W [MeV]	37	30	15	15	15	6
δm_t [GeV]	5.1	4	2	2	0.2	0.13
δM_H [MeV]	—	—	2000	100	50	50

electroweak observables at the Tevatron (Run IIA and IIB), the LHC, a future linear collider, LC, and GigaZ are summarized in Table 1.

In this talk, we discuss the potential impact of high precision measurements of $\sin^2\theta_{\text{eff}}$, M_W , and other observables on the (indirect) determination of the Higgs boson mass in the SM and of non-SM mass scales in the MSSM. These unknown mass scales affect the predictions of the precision observables through loop corrections.

2 Higgs Sector of the SM

Within the SM, the precision observables measured at the Z peak are affected by two high mass scales: the top quark mass, m_t , and the Higgs boson mass, M_H . They enter into various relations between electroweak observables. For example, the radiative corrections entering the relation between M_W and M_Z , and between M_Z and $\sin^2\theta_{\text{eff}}$, have a strong quadratic dependence on m_t and a logarithmic dependence on M_H . We mainly focus on the two electroweak observables that are expected to be measurable with the highest accuracy at GigaZ, M_W and $\sin^2\theta_{\text{eff}}$. The current theoretical uncertainties [5] are dominated by the parametric uncertainties from the errors in the input parameters m_t (see Table 1) and $\Delta\alpha$. The latter denotes the QED-induced shift in the fine structure constant, $\alpha \rightarrow \alpha(M_Z)$, originating from charged-lepton and light-quark photon vacuum polarization diagrams. The hadronic

contribution to $\Delta\alpha$ currently introduces an uncertainty of $\delta\Delta\alpha = \pm 2 \times 10^{-4}$ [6]. Forthcoming low-energy e^+e^- annihilation experiments may reduce this uncertainty to about $\pm 5 \times 10^{-5}$ [7]. Combining this value with future (indistinguishable) errors from unknown higher order corrections, we assign the total uncertainty of $\delta\Delta\alpha = \pm 7 \times 10^{-5}$ to $\Delta\alpha$. For the future theoretical uncertainties from unknown higher-order corrections (including the uncertainties from $\delta\Delta\alpha$) we assume,

$$\delta M_W(\text{theory}) = \pm 3 \text{ MeV}, \quad \delta \sin^2 \theta_{\text{eff}}(\text{theory}) = \pm 3 \times 10^{-5} \quad (\text{future}). \quad (4)$$

Given the high precision of GigaZ, also the experimental error in M_Z , $\delta M_Z = \pm 2.1 \text{ MeV}$, results in non-negligible uncertainties of $\delta M_W = \pm 2.5 \text{ MeV}$ and $\delta \sin^2 \theta_{\text{eff}} = \pm 1.4 \times 10^{-5}$. The experimental error in the top-quark mass, $\delta m_t = \pm 130 \text{ MeV}$, induces further uncertainties of $\delta M_W = \pm 0.8 \text{ MeV}$ and $\delta \sin^2 \theta_{\text{eff}} = \pm 0.4 \times 10^{-5}$. Thus, while currently the experimental error in M_Z can safely be neglected, for the GigaZ precision it will actually induce an uncertainty in the prediction of $\sin^2 \theta_{\text{eff}}$ that is larger than its experimental error.

- The relation between $\sin^2 \theta_{\text{eff}}$ and M_Z can be written as,

$$\sin^2 \theta_{\text{eff}} \cos^2 \theta_{\text{eff}} = \frac{A^2}{M_Z^2(1 - \Delta r_Z)}, \quad (5)$$

where $A = [(\pi\alpha)/(\sqrt{2}G_F)]^{1/2} = 37.2805(2) \text{ GeV}$ is a combination of two precisely known low-energy coupling constants, the Fermi constant, G_F , and the electromagnetic fine structure constant, α . The quantity Δr_Z summarizes the loop corrections, which at the one-loop level can be decomposed as,

$$\Delta r_Z = \Delta\alpha - \Delta\rho^t + \Delta r_Z^H + \dots \quad (6)$$

The leading top contribution to the ρ parameter [8], quadratic in m_t , reads,

$$\Delta\rho^t = \frac{3G_F m_t^2}{8\pi^2 \sqrt{2}}. \quad (7)$$

The Higgs boson contribution is screened and logarithmic for large Higgs boson masses,

$$\Delta r_Z^H = \frac{G_F M_W^2}{8\pi^2 \sqrt{2}} \frac{1 + 9s_W^2}{3c_W^2} \log \frac{M_H^2}{M_W^2} + \dots \quad (8)$$

- An independent analysis can be based on the precise measurement of M_W near threshold. The M_W - M_Z interdependence is given by,

$$\frac{M_W^2}{M_Z^2} \left(1 - \frac{M_W^2}{M_Z^2} \right) = \frac{A^2}{M_Z^2(1 - \Delta r)}, \quad (9)$$

where the quantum correction Δr has the one-loop decomposition,

$$\Delta r = \Delta\alpha - \frac{c_W^2}{s_W^2} \Delta\rho^t + \Delta r^H + \dots, \quad (10)$$

$$\Delta r^H = \frac{G_F M_W^2}{8\pi^2 \sqrt{2}} \frac{11}{3} \log \frac{M_H^2}{M_W^2} + \dots, \quad (11)$$

with $\Delta\alpha$ and $\Delta\rho^t$ as introduced above.

Due to the different dependences of $\sin^2 \theta_{\text{eff}}$ and M_W on m_t and M_H , the high precision measurements of these quantities at GigaZ (and other observables entering a global analysis) can determine m_t and M_H . The expected accuracy in the indirect determination of M_H from the radiative corrections within the SM is displayed in Fig. 1. To obtain these contours, the error projections in Table 1 are supplemented by central values equal to the current SM best fit values for the entire set of current high precision observables [9]. For the theoretical uncertainties, Eq. (4) is used, while the parametric uncertainties, such as from α_s and M_Z , are automatically accounted for in the fits¹. The allowed bands in the m_t – M_H plane for the GigaZ accuracy are shown separately for $\sin^2 \theta_{\text{eff}}$ and M_W . By adding the information on the top-quark mass, with $\delta m_t \lesssim 130$ MeV obtained from measurements of the $t\bar{t}$ production cross section near threshold, an accurate determination of the Higgs boson mass becomes feasible, from both, M_W and $\sin^2 \theta_{\text{eff}}$. If the two values are found to be consistent, they can be combined and compared to the Higgs boson mass measured in direct production through Higgs-strahlung [12] (see the last row in Table 1). In Fig. 1 this is shown by the shaded area, where the measurements of other Z boson properties as anticipated for GigaZ are also included. For comparison, the area corresponding to current experimental accuracies is also shown.

The results can be summarized by calculating the accuracy with which M_H can be determined indirectly. The expectations for $\delta M_H/M_H$ in each step until GigaZ are collected in Table 2. It is apparent that GigaZ, reaching $\delta M_H/M_H = \pm 7\%$, triples the precision in M_H relative to the anticipated LHC status. On the other hand, a linear collider without the high luminosity option would provide only a modest improvement.

- A direct formal relation between M_W and $\sin^2 \theta_{\text{eff}}$ can be established by combining the two relations (5) and (9) as,

$$M_W^2 = \frac{A^2}{\sin^2 \theta_{\text{eff}} (1 - \Delta r_W)}. \quad (12)$$

¹All fit results in this Section were obtained using GAPP [11].

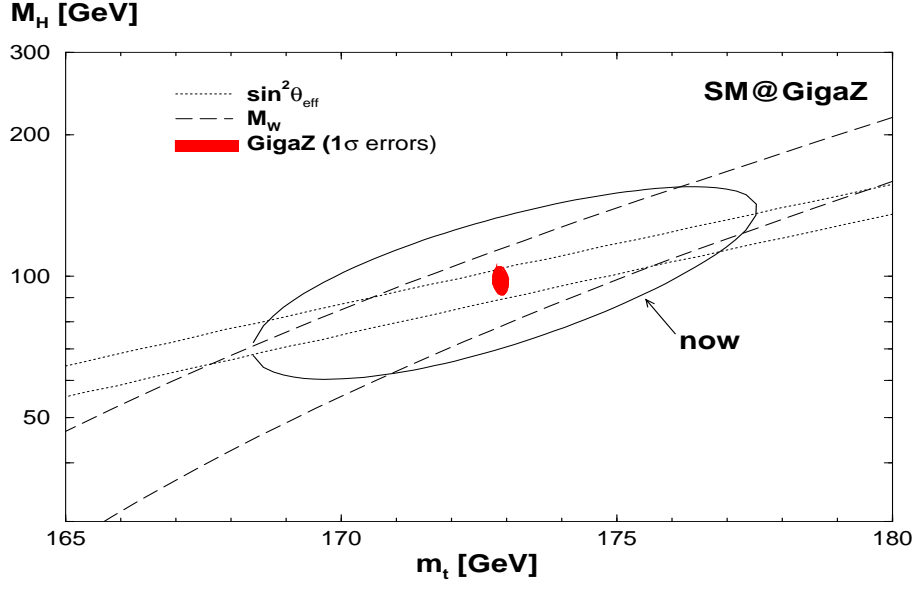


Figure 1: 1σ allowed regions in the m_t - M_H plane taking into account the current measurements and the anticipated GigaZ precisions for $\sin^2 \theta_{\text{eff}}$, M_W , Γ_Z , R_l , R_q and m_t (see text).

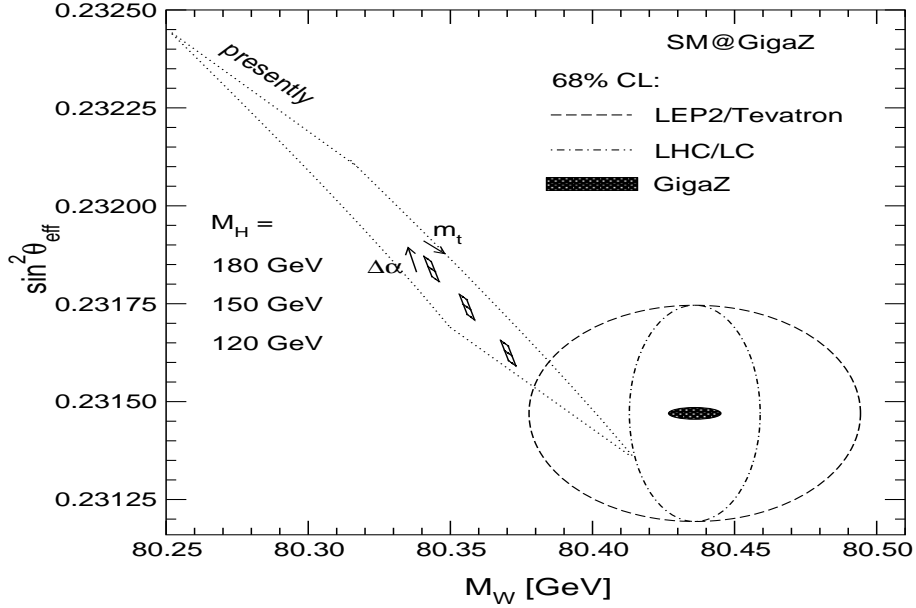


Figure 2: The theoretical prediction for the relation between $\sin^2 \theta_{\text{eff}}$ and M_W in the SM for Higgs boson masses in the intermediate range is compared to the experimental accuracies at LEP 2/Tevatron (Run IIA), LHC/LC and GigaZ (see Table 1). For the theoretical prediction an uncertainty of $\delta \Delta \alpha = \pm 7 \times 10^{-5}$ and $\delta m_t = \pm 200$ MeV is taken into account.

Table 2: *Cumulative* expected precisions of indirect Higgs mass determinations, given the error projections in Table 1. Theoretical uncertainties and their correlated effects on M_W and $\sin^2 \theta_{\text{eff}}$ are taken into account (see text). The last column shows the indirect Higgs mass determination from the full set of precision observables.

	M_W	$\sin^2 \theta_{\text{eff}}$	all
now	200 %	62 %	60 %
Tevatron Run IIA	77 %	46 %	41 %
Tevatron Run IIB	39 %	28 %	26 %
LHC	28 %	24 %	21 %
LC	18 %	20 %	15 %
GigaZ	12 %	7 %	7 %

The quantum correction Δr_W is independent of $\Delta \rho^t$ in leading order and has the one-loop decomposition,

$$\Delta r_W = \Delta \alpha - \Delta r_W^H + \dots, \quad (13)$$

$$\Delta r_W^H = \frac{G_F M_Z^2}{24\pi^2 \sqrt{2}} \log \frac{M_H^2}{M_W^2} + \dots. \quad (14)$$

Relation (12) can be evaluated by inserting the measured value of the Higgs boson mass as predetermined at the LHC and the LC. This is visualized in Fig. 2, where the present and future theoretical predictions for $\sin^2 \theta_{\text{eff}}$ and M_W (for different values of M_H) are compared with the experimental accuracies at various colliders. Besides the independent predictions of $\sin^2 \theta_{\text{eff}}$ and M_W within the SM, the $M_W - \sin^2 \theta_{\text{eff}}$ contour plot in Fig. 2 can be interpreted as an additional indirect determination of M_W from the measurement of $\sin^2 \theta_{\text{eff}}$. Given the expected negligible error in M_H , this results in an uncertainty of

$$\delta M_W(\text{indirect}) \approx \pm 2 \text{ MeV} \pm 3 \text{ MeV}. \quad (15)$$

The first uncertainty reflects the experimental error in $\sin^2 \theta_{\text{eff}}$, while the second is the theoretical uncertainty discussed above (see Eq. (4)). The combined uncertainty of this indirect prediction is about the same as the one of the SM prediction according to Eq. (9) and is close to the experimental error expected from the W^+W^- threshold given in Eq. (2).

Consistency of all the theoretical relations with the experimental data would be the ultimate precision test of the SM based on quantum fluctuations. The comparison between theory and experiment can also be exploited to constrain possible physics

scales beyond the SM. These additional contributions can conveniently be described in terms of the S,T,U [13] or ϵ parameters [14]. Adopting the notation of Ref. [9], the errors with which they can be measured at GigaZ are given as follows:

$$\begin{aligned}\Delta S &= \pm 0.05, & \Delta \hat{\epsilon}_3 &= \pm 0.0004, \\ \Delta T &= \pm 0.06, & \Delta \hat{\epsilon}_1 &= \pm 0.0005, \\ \Delta U &= \pm 0.04, & \Delta \hat{\epsilon}_2 &= \pm 0.0004.\end{aligned}\tag{16}$$

The oblique parameters in Eq. (16) are strongly correlated. On the other hand, many types of new physics predict $U = \hat{\epsilon}_2 = 0$ or very small (see Ref.[9] and references therein). With the U ($\hat{\epsilon}_2$) parameter known, the anticipated errors in S and T would decrease to about ± 0.02 , while the errors in $\hat{\epsilon}_1$ and $\hat{\epsilon}_3$ would be smaller than ± 0.0002 .

3 Supersymmetry

We now assume that supersymmetry would be discovered at LEP 2, the Tevatron, or the LHC, and further explored at an e^+e^- linear collider. The high luminosity expected at TESLA can be exploited to determine supersymmetric particle masses and mixing angles with errors from $\mathcal{O}(1\%)$ down to one per mille, provided they reside in the kinematical reach of the collider, which we assume to be about 1 TeV.

In contrast to the Higgs boson mass in the SM, the lightest \mathcal{CP} -even MSSM Higgs boson mass, M_h , is not a free parameter but can be calculated from the other SUSY parameters. In the present analysis, the currently most precise result based on Feynman-diagrammatic methods [15] is used, relating M_h to the pseudoscalar Higgs boson mass, M_A . The numerical evaluation has been performed with the Fortran code *FeynHiggs* [16]. Later in our analysis we also assume a future uncertainty in the theoretical prediction of M_h of ± 0.5 GeV.

The relation between M_W and $\sin^2 \theta_{\text{eff}}$ is affected by the parameters of the supersymmetric sector, especially the \tilde{t} -sector. At the LHC and in the first phase of LC operations, the mass of the light \tilde{t} , $m_{\tilde{t}_1}$, and the \tilde{t} -mixing angle, $\theta_{\tilde{t}}$, may be measurable very well, particularly in the process $e^+e^- \rightarrow \tilde{t}_1 \bar{\tilde{t}}_1$ (see the last paper of Ref. [1] and references therein). On the other hand, background problems at the LHC and lacking energy at the LC may preclude the analysis of the heavy \tilde{t} -particle, \tilde{t}_2 .

In Fig. 3 we show in a first step of the analysis the effect of the precise determination of $\sin^2 \theta_{\text{eff}}$ alone on the indirect determination of the heavier \tilde{t} mass, $m_{\tilde{t}_2}$. In this first step we neglect the variation of the SUSY parameters and the theoretical uncertainty of M_h . For the precision observables we have taken $\sin^2 \theta_{\text{eff}} = 0.23140$ and $M_h = 115$ GeV with the experimental errors given in the last column of Table 1. For $\tan \beta$, the ratio of the vacuum expectation values of the two Higgs doublets in the MSSM, we assume a relatively well determined $\tan \beta = 3 \pm 0.5$, as can be expected

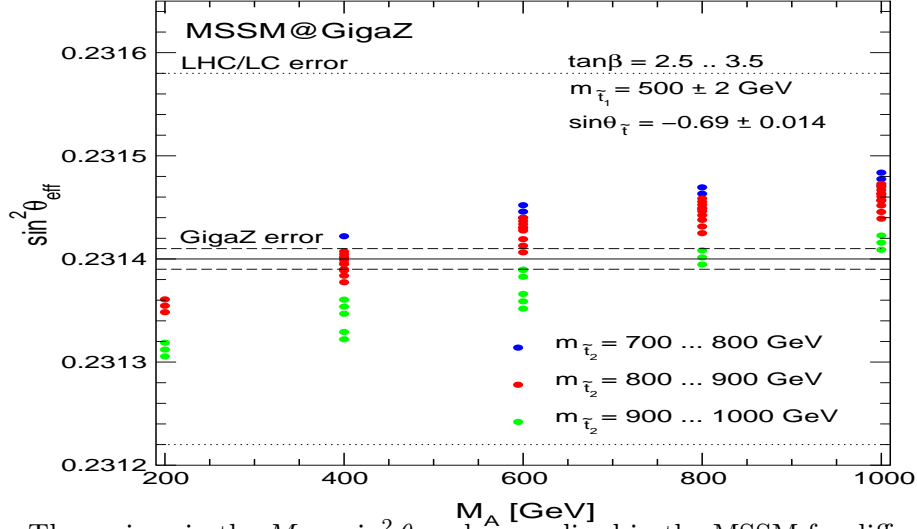


Figure 3: The regions in the $M_A - \sin^2 \theta_{\text{eff}}$ plane realized in the MSSM for different values of $m_{\tilde{t}_2}$. The precision on $\sin^2 \theta_{\text{eff}}$ obtainable at the LHC and the LC is compared to the prospective GigaZ precision around the value $\sin^2 \theta_{\text{eff}} = 0.23140$, for $2.5 < \tan \beta < 3.5$ and the other experimental values as in Fig. 4. (See text for details.)

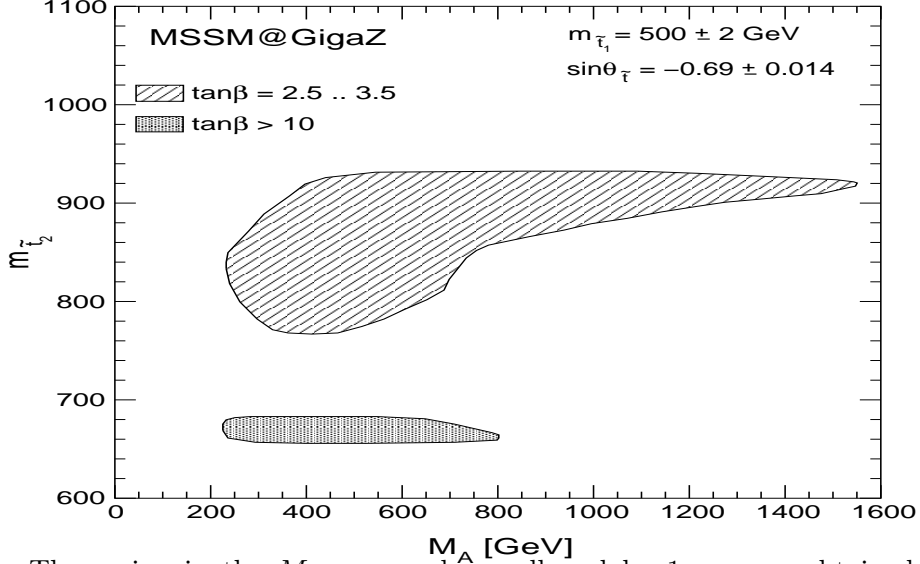


Figure 4: The region in the $M_A - m_{\tilde{t}_2}$ plane, allowed by 1σ errors obtained from the GigaZ measurements of M_W and $\sin^2 \theta_{\text{eff}}$: $M_W = 80.40$ GeV, $\sin^2 \theta_{\text{eff}} = 0.23140$, and from the LC measurement of M_h : $M_h = 115$ GeV. The experimental errors for the SM parameters are given in Table 1. $\tan \beta$ is assumed to be experimentally constrained by $2.5 < \tan \beta < 3.5$ or $\tan \beta > 10$. The other parameters including their uncertainties are given by $m_{\tilde{t}_1} = 500 \pm 2$ GeV, $\sin \theta_{\tilde{t}} = -0.69 \pm 2\%$, $A_b = A_t \pm 10\%$, $\mu = -200 \pm 1$ GeV, $M_2 = 400 \pm 2$ GeV and $m_{\tilde{g}} = 500 \pm 10$ GeV. For the uncertainties of the theoretical predictions we use Eq. (4).

from measurements in the gaugino sector (see e.g. Ref. [17]). As for the other parameters, the following values are assumed: $m_{\tilde{t}_1} = 500 \pm 2$ GeV, $\sin \theta_{\tilde{t}} = -0.69 \pm 2\%$, $A_b = A_t$, $\mu = -200$ GeV, $M_2 = 400$ GeV and $m_{\tilde{g}} = 500$ GeV. ($A_{b,t}$ are trilinear soft SUSY-breaking parameters, μ is the Higgs mixing parameter, M_2 is one of the soft SUSY-breaking parameter in the gaugino sector, and $m_{\tilde{g}}$ denotes the gluino mass.) In Fig. 3 the GigaZ precision for $\sin^2 \theta_{\text{eff}}$ is compared to the precision obtainable at the LHC and a LC without the GigaZ option. While the LHC/LC precision gives no restrictions for $m_{\tilde{t}_2}$ or M_A , the high GigaZ precision could give lower and *upper* bounds on both non-SM mass parameters.

However, a more realistic scenario includes the other precision observable that can be determined at GigaZ with extremely high precision, M_W . In addition, all uncertainties of the additional SUSY mass scales, as well as the theoretical uncertainty of the Higgs boson mass prediction have to be taken into account. Therefore, as a second step in our analysis we now consider $\sin^2 \theta_{\text{eff}}$ and M_W and include all possible uncertainties. It is demonstrated in Fig. 4 how in this complete analysis limits on $m_{\tilde{t}_2}$ and M_A can be derived from measurements of M_h , M_W , and $\sin^2 \theta_{\text{eff}}$. As experimental values we assumed $M_h = 115$ GeV, $M_W = 80.40$ GeV, and $\sin^2 \theta_{\text{eff}} = 0.23140$, with the experimental errors given in the last column of Table 1, and the future theoretical uncertainty for the Higgs boson mass of ± 0.5 GeV. We now consider two cases for $\tan \beta$: the low $\tan \beta$ region, where we assume a band, $2.5 < \tan \beta < 3.5$ as for Fig. 3, and the high $\tan \beta$ region where we assume a lower bound, $\tan \beta \geq 10$ (see e.g. Ref. [17] and references therein). As for the other parameters, the following values are assumed, with uncertainties as expected from LHC and TESLA: $m_{\tilde{t}_1} = 500 \pm 2$ GeV, $\sin \theta_{\tilde{t}} = -0.69 \pm 2\%$, $A_b = A_t \pm 10\%$, $\mu = -200 \pm 1$ GeV, $M_2 = 400 \pm 2$ GeV and $m_{\tilde{g}} = 500 \pm 10$ GeV.

In this full analysis, taking into account all possible uncertainties, for low $\tan \beta$ the heavier \tilde{t} -mass, $m_{\tilde{t}_2}$, can be restricted to $760 \text{ GeV} \lesssim m_{\tilde{t}_2} \lesssim 930 \text{ GeV}$. The mass M_A varies between 200 GeV and 1600 GeV. A reduction of this interval to $M_A \geq 500$ GeV by its non-observation at the LHC and the LC does not improve the bounds on $m_{\tilde{t}_2}$. If $\tan \beta \geq 10$, the allowed region turns out to be much smaller ($660 \text{ GeV} \lesssim m_{\tilde{t}_2} \lesssim 680 \text{ GeV}$), and M_A is restricted to $M_A \lesssim 800$ GeV.

In deriving the bounds on $m_{\tilde{t}_2}$, both the constraints from M_h (see Ref. [18]) and $\sin^2 \theta_{\text{eff}}$ play an important role. For the bounds on M_A , the main effect comes from $\sin^2 \theta_{\text{eff}}$. We have assumed a value for $\sin^2 \theta_{\text{eff}}$ slightly different from the corresponding value obtained in the SM limit. For this value the (logarithmic) dependence on M_A (see also Fig. 3) is still large enough so that in combination with the high precision in $\sin^2 \theta_{\text{eff}}$ at GigaZ an *upper limit* on M_A can be set. For an error as obtained at an LC without the GigaZ mode (see Table 1) no bound on M_A could be inferred. Thus, the high precision measurements of M_W , $\sin^2 \theta_{\text{eff}}$, and M_h do not improve the direct lower bound on the mass of the pseudoscalar Higgs boson A , but instead they enable us to set an *upper bound*.

4 Conclusions

The opportunity to measure electroweak observables very precisely in the GigaZ mode of the projected e^+e^- linear collider TESLA, in particular the electroweak mixing angle $\sin^2 \theta_{\text{eff}}$ and the W boson mass, opens new areas for high precision tests of electroweak theories. We have analyzed in detail two examples: (i) The Higgs mass of the Standard Model can be extracted to a precision of a few percent from loop corrections. By comparison with the direct measurements of the Higgs mass, bounds on new physics scales can be inferred that may not be accessible directly. (ii) The masses of particles in supersymmetric theories, which for various reasons may not be accessible directly neither at the LHC nor at the LC, can be constrained. Typical examples are the heavy scalar top quark and the mass of the \mathcal{CP} -odd Higgs boson, M_A . (Further examples for the MSSM have also been studied in the original literature [1].) In the scenarios studied here, a sensitivity of up to order 2 TeV for the mass of the pseudoscalar Higgs boson and an upper bound of about 1 TeV for the heavy scalar top quark can be expected. Opening windows to unexplored energy scales renders these analyses of virtual effects an important tool for experiments in the GigaZ mode of a future e^+e^- linear collider.

Acknowledgments

It is a pleasure for J.E. to thank the organizers for a very pleasant conference in a spectacular setting.

References

- [1] See S. Heinemeyer, T. Mannel and G. Weiglein, e-print [hep-ph/9909538](#);
J. Erler, S. Heinemeyer, W. Hollik, G. Weiglein, and P.M. Zerwas, *Phys. Lett.* **B486** (2000) 125;
S. Heinemeyer and G. Weiglein, e-print [hep-ph/0012364](#); and references therein.
- [2] A. Blondel, *Phys. Lett.* **B202** (1988) 145.
- [3] R. Hawking and K. Mönig, *EPJdirect* **C8** (1999) 1;
K. Mönig, e-print [hep-ex/0101005](#).
- [4] G. Wilson, Proceedings, Linear Collider Workshop, Sitges 1999.
- [5] D. Bardin, M. Grünewald and G. Passarino, e-print [hep-ph/9802452](#).

- [6] M. Davier and A. Höcker, *Phys. Lett.* **B435** (1998) 427;
J. Kühn and M. Steinhauser, *Phys. Lett.* **B437** (1998) 425;
J. Erler, *Phys. Rev.* **D59** (1999) 054008;
F. Jegerlehner, e-print [hep-ph/9901386](#).
- [7] F. Jegerlehner, *The effective fine structure constant at TESLA energies*, LC-TH-2001-035.
- [8] M. Veltman, *Nucl. Phys.* **B123** (1977) 89.
- [9] J. Erler and P. Langacker, in Ref. [10].
- [10] D.E. Groom *et al.*, *Eur. Phys. J.* **C15** (2000) 1.
- [11] J. Erler, e-print [hep-ph/0005084](#).
- [12] J. Ellis, M. Gaillard and D. Nanopoulos, *Nucl. Phys.* **B106** (1976) 292;
B. Ioffe and V. Khoze, *Sov. J. Part. Nucl.* **9** (1978) 50;
B. Lee, C. Quigg and H. Thacker, *Phys. Rev.* **D16** (1977) 1519;
V. Barger, K. Cheung, A. Djouadi, B. Kniehl and P. Zerwas, *Phys. Rev.* **D49** (1994) 79.
- [13] M. Peskin and T. Takeuchi, *Phys. Rev.* **D46**, 381 (1992).
- [14] G. Altarelli and R. Barbieri, *Phys. Lett.* **B253**, 161 (1990).
- [15] S. Heinemeyer, W. Hollik and G. Weiglein, *Phys. Rev.* **D58** (1998) 091701; *Phys. Lett.* **B440** (1998) 296; *Eur. Phys. J.* **C9** (1999) 343.
- [16] S. Heinemeyer, W. Hollik and G. Weiglein, *Comp. Phys. Comm.* **124** (2000) 76; e-print [hep-ph/0002213](#).
- [17] S.Y. Choi, A. Djouadi, M. Guchait, J. Kalinowski, and P.M. Zerwas, *Eur. Phys. J.* **C14**, (2000) 535.
- [18] G. Weiglein, e-print [hep-ph/0001044](#).